IEEE Access
Multidisciplinary | Rapid Review | Open Access Journal

Received October 7, 2021, accepted October 21, 2021, date of publication October 26, 2021, date of current version November 8, 2021.

Digital Object Identifier 10.1109/ACCESS.2021.3122915

Investigations of AE Signals Emitted From Dropped Indenter on Steel Pipes' Surface

MOHAMED SHEHADEH[1,2], AHMED OSMAN[1], ALY HASSAN ABDELBAKY ELBATRAN[1], J. A. STEEL[2], AND R. L. REUBEN[2]

[1]Marine Engineering Department, College of Engineering and Technology, Arab Academy of Science, Technology and Maritime Transport, Alexandria 21913, Egypt

[2]Department of Mechanical Engineering, School of Engineering and Physical Sciences, Heriot-Watt University, Edinburgh EH14 4AS, U.K.

Corresponding author: Ahmed Osman (ahmed.osman@aast.edu)

ABSTRACT Acoustic emission (AE) are stress waves created by the material deformation, which could be utilized to detect impacts of objects within different mechanical systems. In a mechanical system, impacts from dropped masses are pertinent to realistic wave sources where is to improve precision of source location in real situation. As such, work is required in order to experimentally evaluate the distortions of AE signals using a set of impacts tests. A series of source intensities were simulated on a steel pipe also the effects of signal type and intensity on the frequency and time domain features were determined. In order to locate and reconstitute the time- and frequency-domain signatures of the AE source, sensors were mounted externally on segments of the tested pipes. It is concluded that the AE energy was easily affected by the location of the indenter shape/geometry. This study demonstrated the significant features and the capability of AE associated with real sources for evaluating and determining the intensity, nature and the position of the damaging events.

INDEX TERMS Acoustic emission, cumulative energy, impact, indentation, sensors, pipeline.

I. INTRODUCTION

AE technique has been demonstrated as an effective method for detecting growing flaws and fatigue in structures by monitoring their AE signals [1]–[8]. AE monitoring technique utilizes the energy released from the structural flaws for its operation and does not require extrinsic energy sources [3] and hence, it is considered as a passive monitoring technique [9], [10]. AE excels over other evaluation methods as the signals are sourced internally from the material itself not from external sources like other non-destructive inspection techniques [11]–[14]. AE also surpasses other monitoring techniques as it is considered as a motion detection technique unlike the material abruption detection that is carried out by other methods [9], [13], [15]. The literature recommended AE method as an efficient technique [4], [16]–[21] for monitoring mechanical systems via structural testing and surveillance [22], machines monitoring and processes control [23], and materials characterization [24]. The AE signals are prone to dispersion and attenuation due to wave elasticity [9], [25]. The majority of studies in the AE monitoring field have investigated substrates of thin-plate form [26]–[30]. Literature that was concerned about higher crack rates and degrees of crack plasticity suggested that the extent of crack tip plasticity becomes indispensable where an increase in the size of the plastic zone occurs [31]–[33] as in low-cycle fatigue or with semi-ductile substrates. Hence, impact could be a significant damage source in different mechanical processes, and AE monitoring for such damage potential is crucial for the safety and establishment of structural systems [34]–[37]. Prosser *et al.* [38] studied the released AE occurred by an impact of two projectile types on an aluminum and graphite/epoxy composites plate. An air gun triggered a steel projectile caused an impact of a low-velocity (0.21 Kms^{-1}). An impact of a higher-velocity (1.80 – 7.00 Kms^{-1}) of a nylon-projectile was triggered from a gas-gun. It was claimed that some evaluation data (differentiation between penetrating and non-penetrating impact events and source-location), could possibly be determined. However, additional work was mandatory to study the effects of the size and material effects of a projectile in addition to its structural-geometry, propagation-distance and its velocity, in order to obtain a credible impact monitoring system for an aircraft. Gaul and Hurlebaus [39] utilized a pendulum impactor on a suspended steel plate to detect the impact source/location using the maximum wavelet-magnitude to determine the arrival-times.

The associate editor coordinating the review of this manuscript and approving it for publication was Qiuye Sun.

Subsequent research work was conducted in the same area [40]. However, this technique is only concerned with source location but disregarding the nature of the impact events. However, Shehadeh et al were concerned with monitoring pipeline bending and bucking using the AE technique (e.g., references [41]–[43]). They used cross correlation with wavelet transform method for the AE source localization in long pipes [44]. The location and reconstitution of the time-domain signatures of AE sources in pipes was established in subsequent tests that utilized a linear array of the AE sensors [3]. The correlation between AE signal attenuation with a discontinuous steel pipe was examined by Shehadeh *et al.* [45]. The distortions of AE continuous as well as the semi-continuous sources in the time and frequency-domains was evaluated. Two different methods have generated simulated, relatively white sources; continuous AE from a compressed air jet, and semi-continuous signals using a solenoid valve to regulate the air jet. The continuous and semi-continuous sources simulate the impact of steel pipes which are investigated and represented in the present study. A novel strategy of a phase array AE localization was introduced by considering the actual trajectory of the propagating elastic waves in order to localize both radial and axial positions of defects [46], [47].

In this study, a series of tests were performed using energy in the time domain methods to acquire the important traits of the AE signals related to un-temporal sources in steel pipe to improve the precision of source location in real situations. The main goal of this work is to research those traits along with an identity of the time and frequency factors the use of simulated and practical sources. Different intensities had been simulated for the duration of the impact tests; and the effect of type and intensity on time and frequency domain features of the source was evaluated.

II. EXPERIMENAL SET UP AND PROCEDURES

Temporal and locative distribution of the AE sources is not very controllable compared to that with simulated sources that were examined in the previous studies [44], [45]. Subsequently, the current study aims to examine the behavior of realistic AE sources. This study developed analytical techniques to gather important traits of the AE signals related to realistic sources. This was achieved using energy in the time domain methods by taking the propagation characteristics established in the aforementioned studies into account. Three experiments were performed to investigate the effects of an indenter of different masses, heights and geometries of on relatively long steel pipes. A series of mass-drop tests were performed with the impact tests as shown in Fig. 1. The pipe was mounted on the rig over two simple supports as shown in Fig. 2, which were sheathed with rubber to eliminate as much potential generated noise from the interaction between the pipe and its supports. Masses with a mass of 5 kg and 10 kg were mounted on an aluminum frame that weighs 1.5 kg on which a steel indenter was mounted and the entire assembly was pushed onto two steel rails from a height up to 1.5 m. The

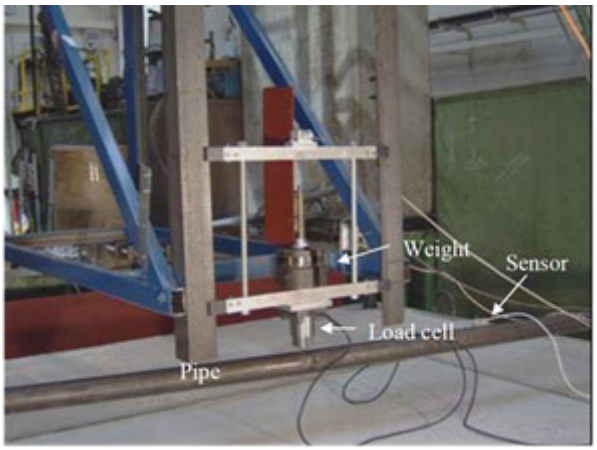

FIGURE 1. Impact test rig assembly.

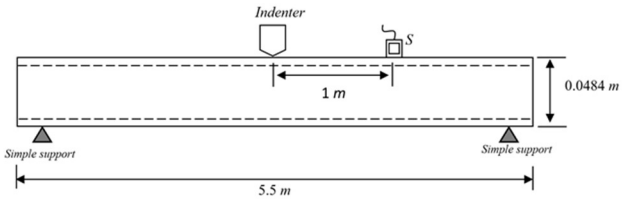

FIGURE 2. Schematic layout of impact test rig.

tests were performed using one sensor which was used in each of these tests and mounted on a steel (ASTM A106/99) pipe of a 5.5 m nominal length, 48.4 mm external diameter, and wall-thickness of 7.35 mm, the sensor is mounted 1 m away from the indenter/source as shown in Fig. 2. Broadband sensors (PAC Micro80D) and PAC-1120A amplifiers were used for AE signal acquisition as in the previous work performed by Sehadeh *et al.* [43].

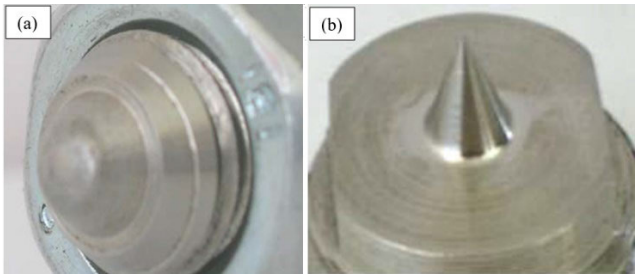

FIGURE 3. (a) Spherical indenter and (b) Conical indenter.

A. SPHERICAL INDENTER TESTS

A spherical indenter of a 6 mm diameter was utilized (Fig. 3a) for the initial test. The test indenter was strain hardened and stabilized into the shape shown after being dropped 3 to 4 times. Each masse of 1.5 kg, 6.5 kg and 11.5 kg was dropped three times from heights of 0.5 m, 1 m and 1.5 m in each test. Assuming that the resulting crater is of a spherical cap geometry, the depth and diameter of the indentation were determined, and the volume was evaluated.

FIGURE 4. An impact crater of 6 mm diameter and 0.83 mm depth on the pipe surface from a 11.5 kg load dropped at 1.5 m height using a spherical indenter.

TABLE 1. Volume (mm^3) of spherical indentation on pipe surface for various masses dropped from multiple heights.

Mass (kg)	Height (m)		
	0.50	1.00	1.50
1.50	Nil	Nil	1.06
6.50	5.30	5.20	5.60
11.50	8.85	9.06	11.90

TABLE 2. Kinetic energies (j) of the dropped masses from specified height (s).

Mass (kg)	Height (m)		
	0.50	1.00	1.50
1.50	7.3	14.7	22
6.50	32	64	95.6
11.50	56.4	113	169

A 240 frames per second high-speed camera was used to determine the kinetic energy (KE) of the carriage and its mass for speed measurement of the 1.5 kg dropped mass from the aforementioned heights [6]. Although the speed of the dropped mass is not affected by its mass from a specific height, the friction in the carriage guideway could create a mass-independent retarding force. This friction could be considered constant for all experiments and could be calculated from the following equation (Eq.1):

$$Fg - F_f = ma \qquad \text{(Eq. 1)}$$

where F_g is the total friction force, Eq2;

$$F_g = g.m; \qquad \text{(Eq. 2)}$$

a is acceleration; and m is the mass of the dropped mass.

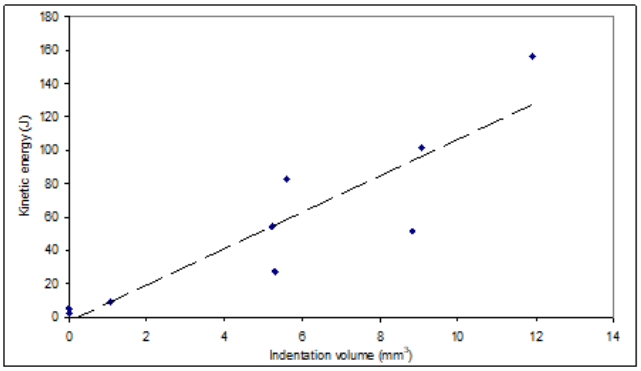

FIGURE 5. Kinetic-energy vs. indentation's surface volume for various masses plopped from multiple levels.

Since the carriage starts from stagnation, the impact velocity, v is given by Eq. 3:

$$v = \sqrt{2as} \qquad \text{(Eq. 3)}$$

and hence the kinetic energy due to impact is (Eq.4):

$$KE = 0.5\, mv^2 \qquad \text{(Eq. 4)}$$

The energy associated with an AE signal over a time, t, can be determined as follows [6]:

$$E = \int_0^t v^2\,(t)\,dt \qquad \text{(Eq. 5)}$$

The AE amplitude [noted as v (t)] in volts, t is time in seconds, and the AE energy is specified in V^2.s.

B. CONICAL INDENTER TESTS

A new conical indenter (Fig. 3b) of 6 mm base diameter and 6.5 mm in height, was employed for the next set of tests. Two masses of 6.5 kg and 11.5 kg have dropped from two heights of 0.5 m and 1 m. The indenters were installed on a load cell (Novatech F218) that could resolve impact loads-up to 40 tons with a time-resolution of 500 Hz [6].

C. INDENTER SHAPE

Another series of tests (five replicates) were carried out to investigate the effects of the indenter geometry on the AE signal features after multiple impact trials. Starting with a conical indenter shape; a mass of 11.5 kg dropped from 1 m height with a single indenter [6].

III. RESULTS AND DISCUSSIONS

The aforementioned tests (three experiments) were performed to investigate the effects of various masses, heights and indenter geometries on a relatively long steel-pipes. Raw signals were acquired at a sampling rate of 5 MHz for a fixed period of 20ms, and the energy content was evaluated using the time domain- and frequency-domain analyses for all of the tests.

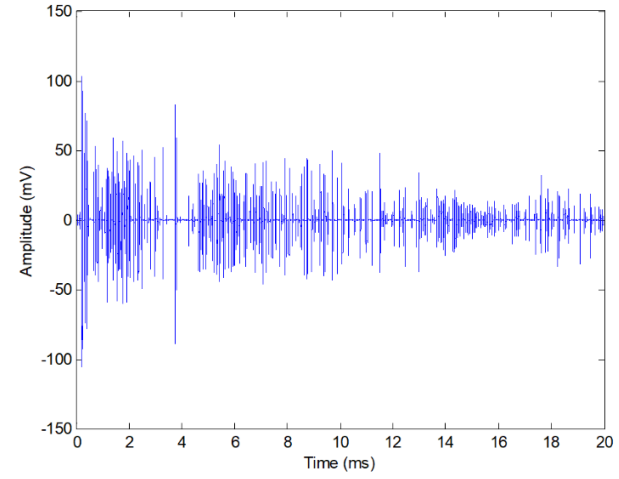

a: 0.5 m

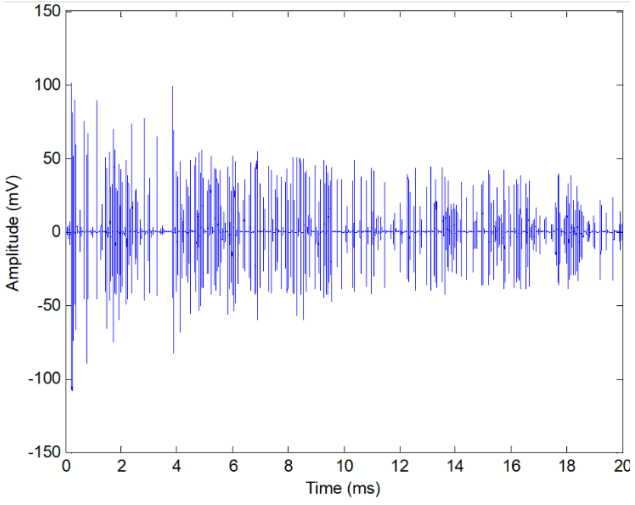

b: 1.0 m

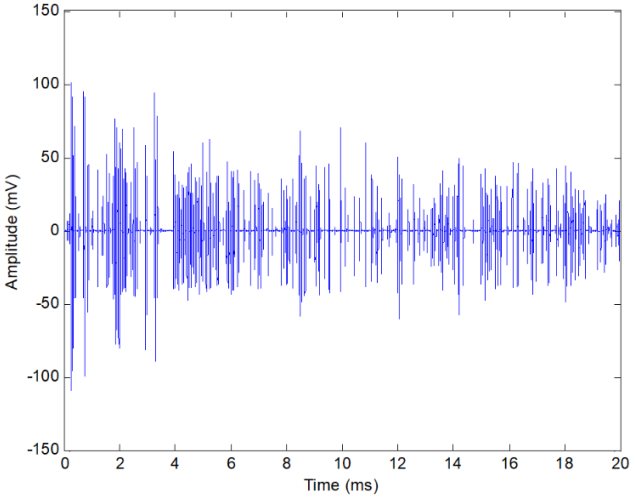

c: 1.5 m

FIGURE 6. AE signal (raw) for 1.5 kg plopped at multiple heights (a = 0.5 m, b = 1.0 m and c = 1.5 m).

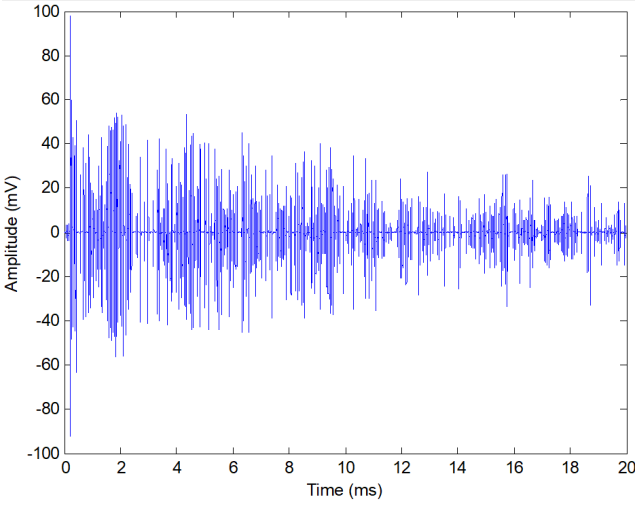

a: 0.5 m

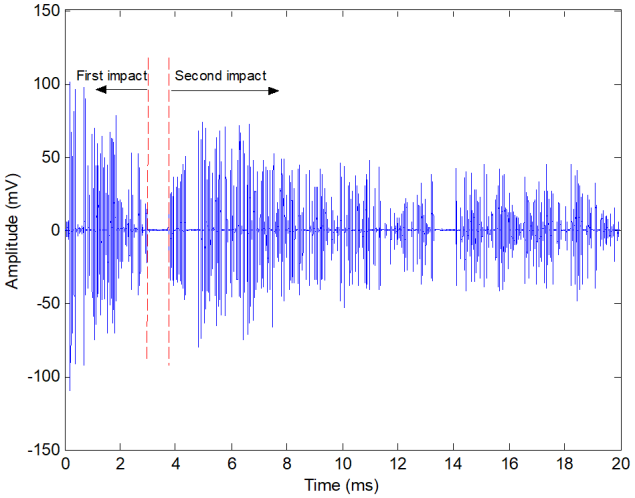

b: 1.0 m

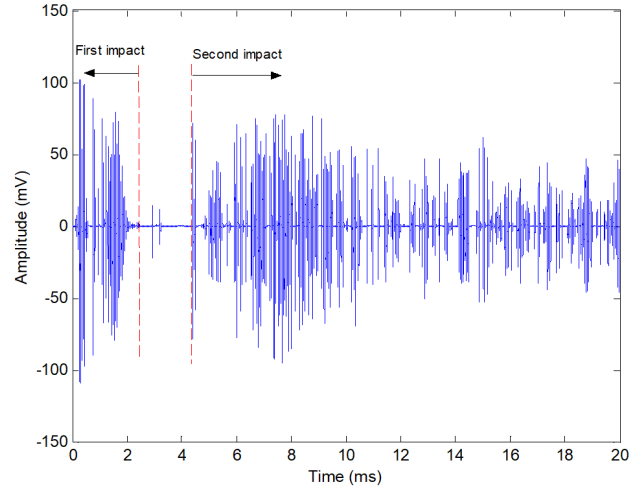

c: 1.5 m

FIGURE 7. AE signal (raw) for 6.5 kg plopped at multiple levels (a = 0.5 m, b = 1.0 m and c = 1.5 m).

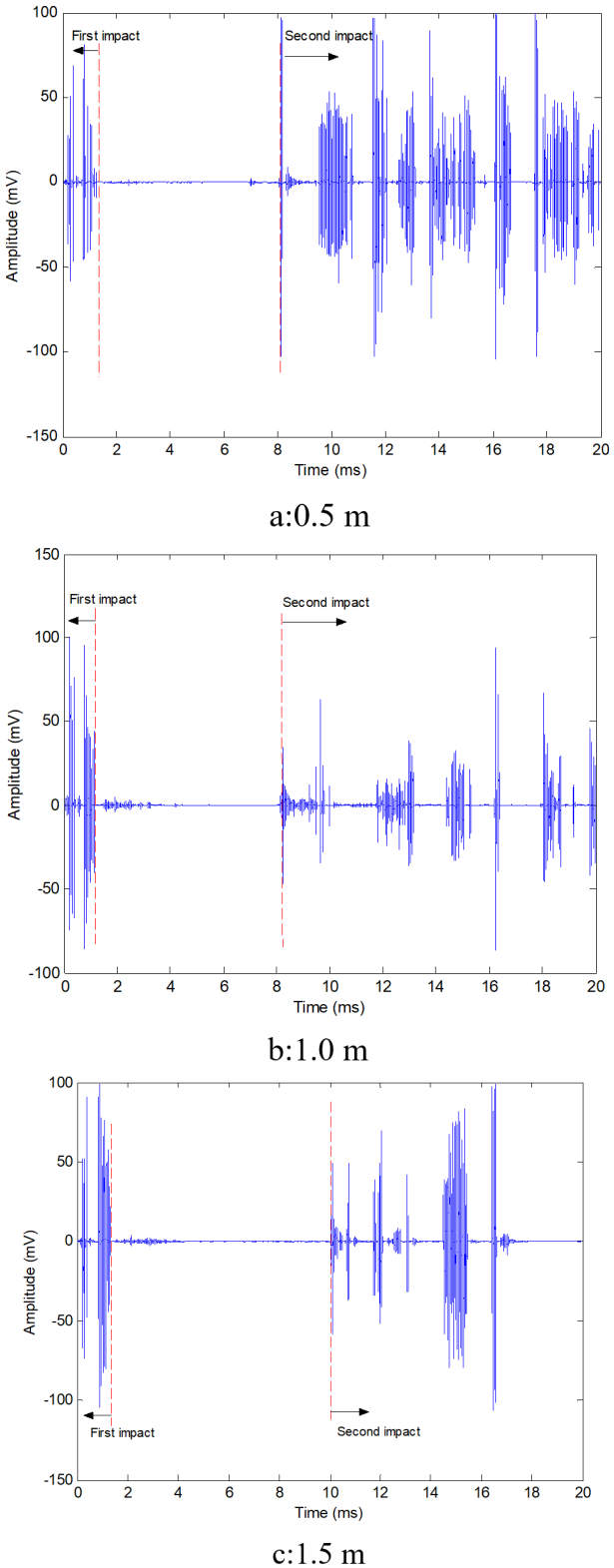

FIGURE 8. AE signal (raw) for 11.5 kg plopped at multiple levels (a = 0.5 m, b = 1.0 m and c = 1.5 m).

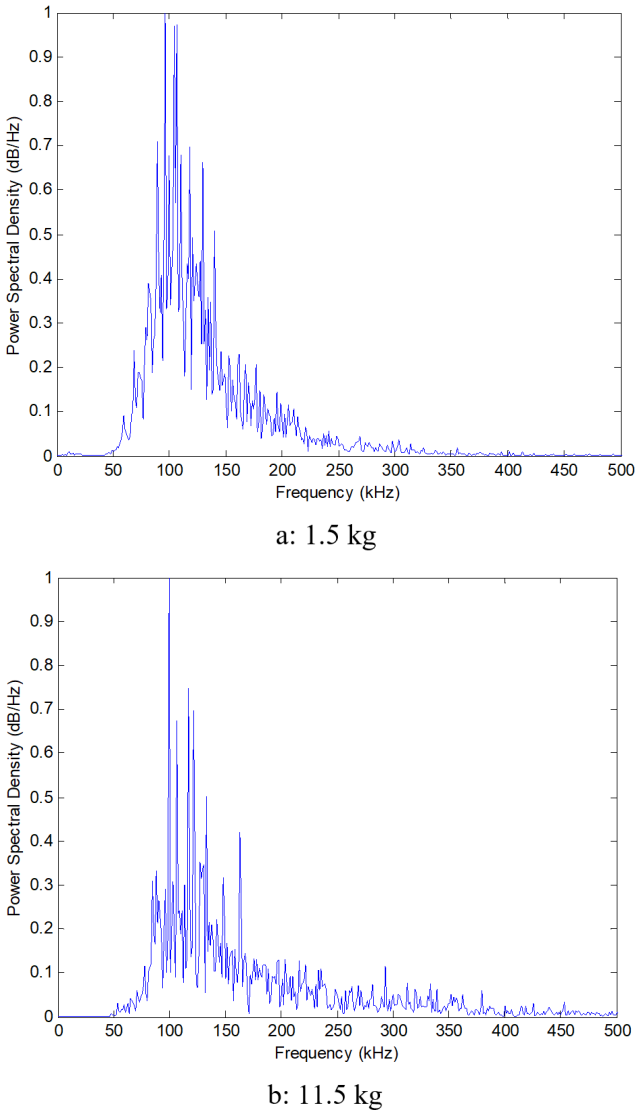

FIGURE 9. Normalized frequency of dropped masses (a: 1.5 kg and b: 11.5 kg) at 1.5 m height.

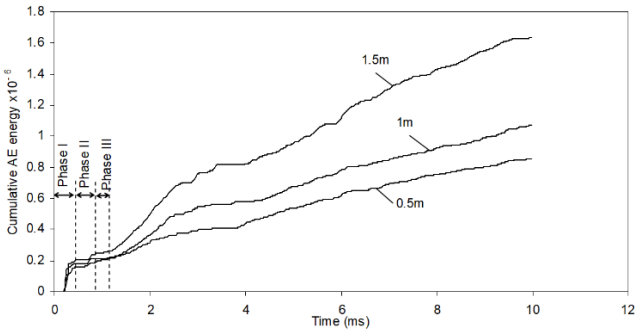

FIGURE 10. AE energy (cumulative) from 1.5 kg plopped mass at multiple levels via a spherical-indenter.

A. SPHERICAL INDENTER TESTS

A single spherical indenter was dropped from multiple heights (0.5, 1.0 and 1.5 m) each using three different masses, each condition being repeated three times on a new location on the pipe surface located 1 m away from the sensor [6]. A typical impact crater on the pipe surface is shown in Fig. 4. Assuming that the resulting crater is of a spherical cap

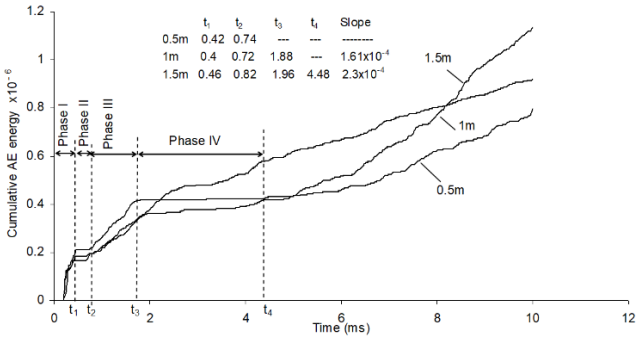

FIGURE 11. AE energy (cumulative) for 6.5 kg plopped mass at different levels via a spherical-indenter.

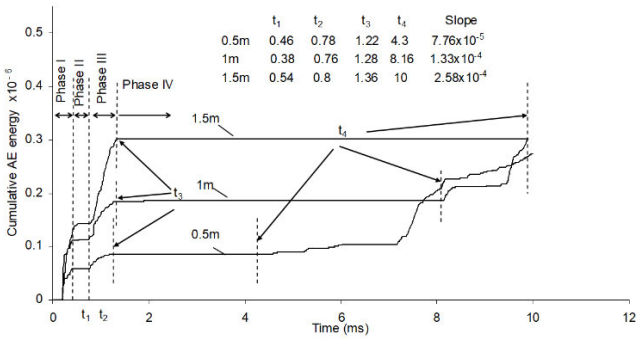

FIGURE 12. AE energy (cumulative) for 11.5 kg plopped mass at multiple levels via a spherical-indenter.

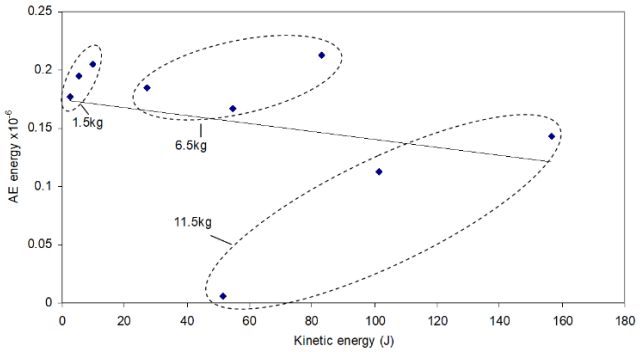

FIGURE 13. Kinetic-energy vs. AE-energy for Phase I and Phase II via a spherical-indenter.

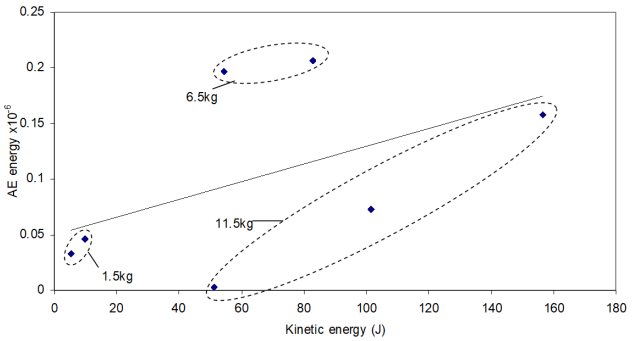

FIGURE 14. Kinetic-energy vs. AE-energy for Phase-III using a spherical-indenter.

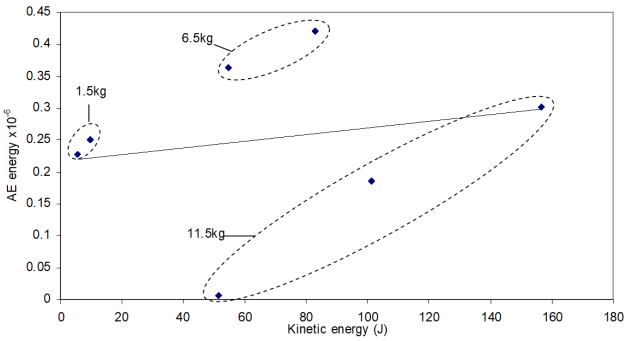

FIGURE 15. Kinetic-energy vs. AE-energy for Phases I - IV via spherical-indenter.

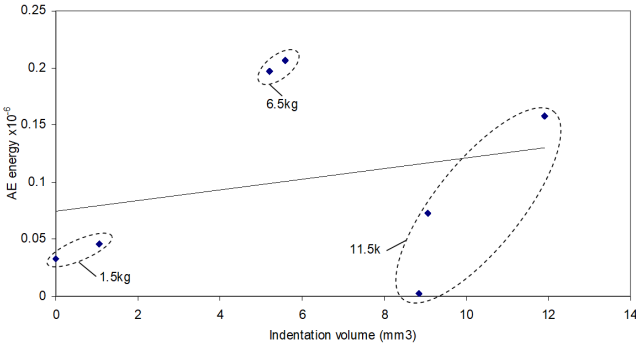

FIGURE 16. Indentation-volume vs. AE-energy for Phase-I and Phase-II via spherical-indenter.

geometry, the indentation dimensions were measured, and the volume was evaluated as shown in Table 1. Deformation was negligible for the 1.5 kg mass dropped from heights of 0.5 m and 1.0 m.

Table 2 shows the calculated magnitudes of the energy due to impact, Eq.4, where no friction losses are assumed. Fig. 5 demonstrates the correlation between the indented volume and the evaluated kinetic-energy of the impact. It was noted that a relationship is existed which the kinetic energy was increased with the increasing of the dropped mass and height.

The raw AE-signals released from the impact tests of the (1.5 kg, 6.5 kg and 11.5 kg) masses dropped at multiple heights are shown in Figs. 6, 7 and 8 respectively. However, it is hard to characterize the initial-impact from the dropped 1.5 kg mass from the all of the aforementioned heights and the dropped 6.5 kg from 0.5 m. A clear gap can be approximately seen for the remainder between 2 ms and a return-time which seems varying with the impact-energy.

Figure 9 demonstrates the AE signals' spectra (normalized) for 1.5 kg as well as the 11.5 kg masses dropped from 1 m. It can be noticed that only a relatively low-broadband frequency-component appeared at nearly 100 KHz.

Analysis of the AE signal variation with time was of interest after the aforementioned results/data was determined. The AE cumulative-energy was evaluated with the aid of discrete elements evaluated over a time-frame of 20μs and the average

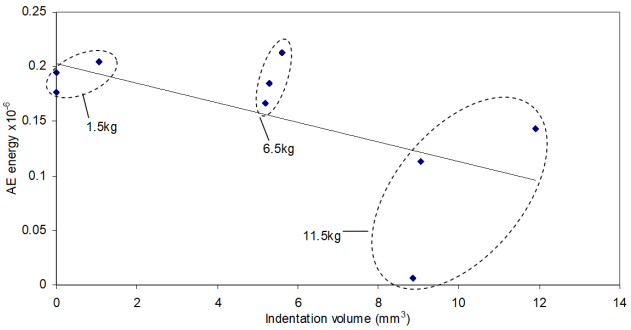

FIGURE 17. Indentation-volume vs. AE-energy for Phase III via spherical-indenter.

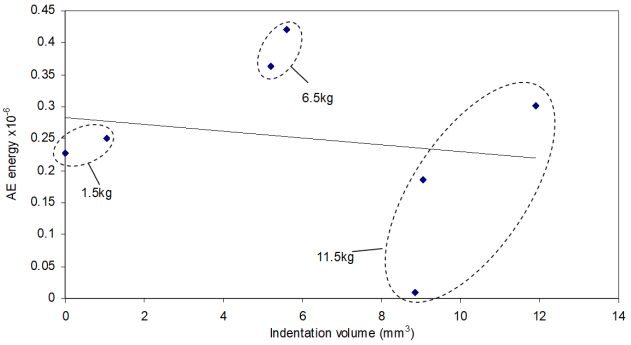

FIGURE 18. Indentation-volume vs. AE-energy for Phases I - IV via spherical-indenter.

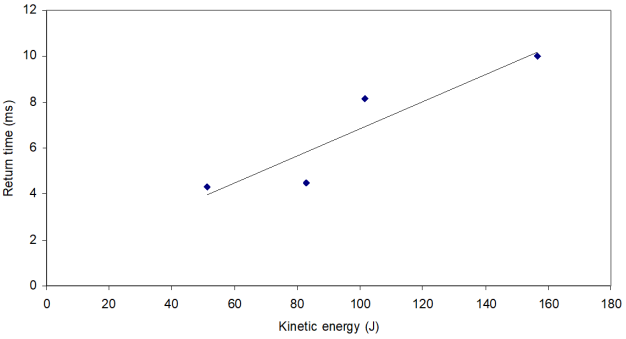

FIGURE 19. Kinetic-energy vs. return-time (t_4) via spherical-indenter.

of the estimated evolutions are plotted in Fig. 10, 11 and 12 for the first 10 ms of the signal. There is obviously an energy stratification for the heaviest mass (Fig. 9). At the initial 10 ms, 4-different-phases being noticeable with boundaries at t1, t2, t3 and t4. These phases are easier to discern as the kinetic energy decreased (Fig. 10 and 11). Figures 10 and 11 demonstrated the return time (t_4) and the AE energy's development slope with respect to time in Phase-III could possibly evaluated from the plots which could for some of the conditions be confirmed.

The initial impact could be assumed to occur during Phase-I and Phase-III while Phase-IV resembles a subsequent impact after ricocheting-off the indenter to the surface and then gets back. Consequently, the energy of Phase-I

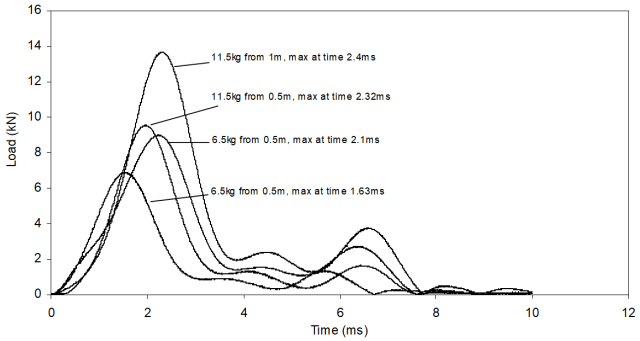

FIGURE 20. Multiple mass loads and levels utilizing conical-indenter.

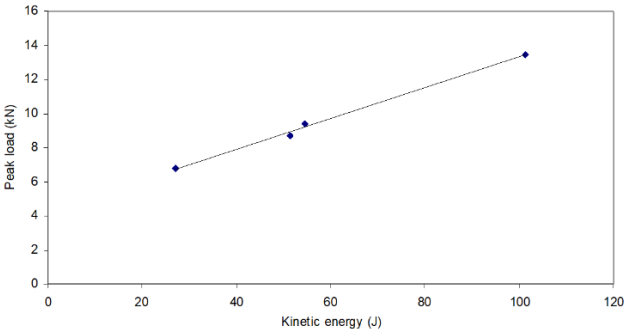

FIGURE 21. Peak load and kinetic-energy via conical-indenter.

and Phase-II, Phase-III and a plot of the three phases is evaluated versus the kinetic-energy of the impact as in Fig. 13 - 15, respectively. However, it was noticed that the data of the plopped 1.5 kg from levels of 0.5 m and 1 m, and 6.5 kg plopped from 0.5 m does not manifest any noticeable phase-separation within these plots. The AE and the kinetic energy are not correlated. For each mass, the AE-energy is influenced by the drop-level independently of the potential or kinetic energies. Equivalently, Fig. 16 to 18 demonstrated the correlation between AE and indentation volume in case of a separately considered masses. However, the return-time (t_4) plotted in Fig. 19, demonstrates an obvious correlation to kinetic-energy for such cases where t4 can be determined. The aforementioned remarks demonstrate the dynamic relationship between the indenter and pipe and that, whilst the AE-energy is probably related to the impact-energy, a perspicuous method of separating the initial impact from recoils needs to be determined.

AE due to impact damage tends to manifest itself mostly in low frequencies and impacts produce signals which can be heavily influenced by the nature of the impact and the dynamic response of the pipe.

B. CONICAL INDENTER TESTS

The conical indenters were utilized for testing two masses and two levels and the load cell in which the indenter was mounted during this test. Consequently, Fig. 20 illustrates the resulting measured forces with respect to the measured time. It also demonstrated that the level of the first peak correlated

FIGURE 22. Conical-indenters after impact, a) 6.5 kg (0.5 m), b) 6.5 kg (1.0 m), c) 11.5 kg (0.5 m) and d) 11.5 kg (1.0 m).

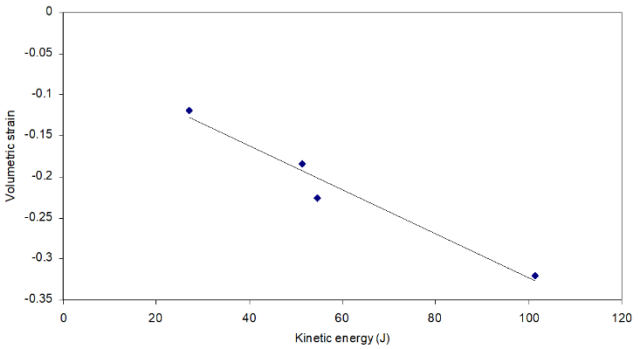

FIGURE 23. Kinetic-energy vs. volumetric-strain via conical-indenter.

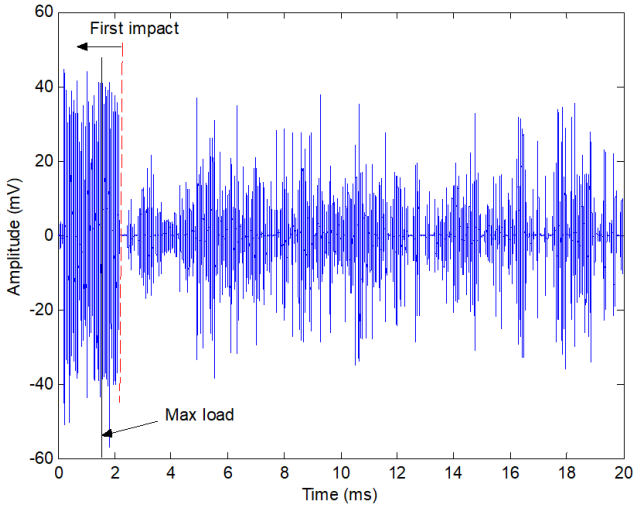

FIGURE 24. AE signal (raw) for 6.5 kg plopped at 0.5 m via conical-indenter.

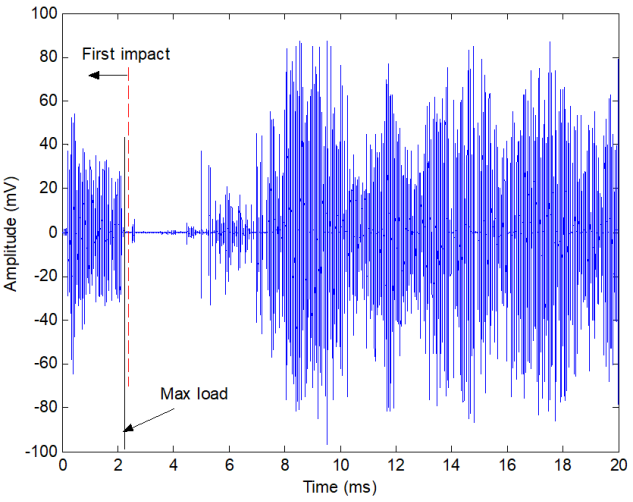

FIGURE 25. AE signal (raw) for 11.5 kg plopped at 1 m via conical-indenter.

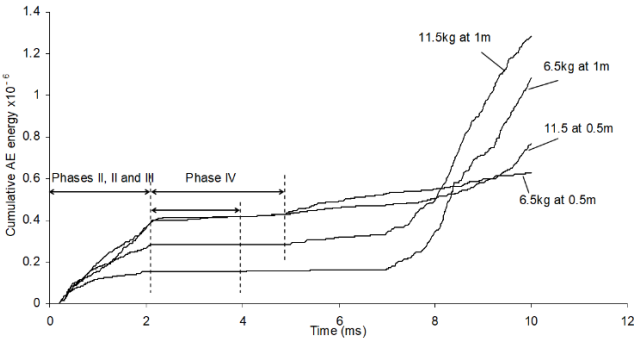

FIGURE 26. AE energy (cumulative) of multiple masses and levels via conical-indenter.

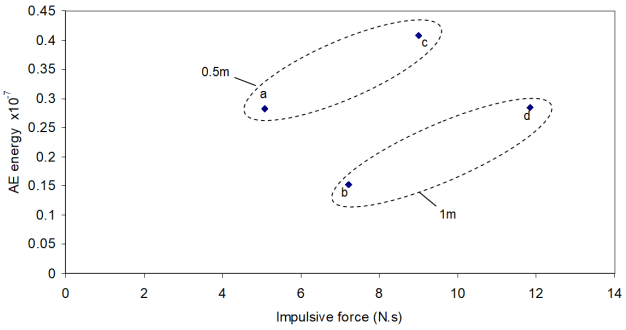

FIGURE 27. AE-energy vs. impulsive-force of Phases I - IV via conical-indenter, a) 6.5 kg (0.5 m), b) 6.5 kg (1.0 m), c) 11.5 kg (0.5 m) and d) 11.5 kg (1.0 m).

to the kinetic-energy of the indenter as shown in Fig. 21. The indentation on the surface was negligible for these tests, in contrast of the less significant of the indenter's deformation as shown in Fig. 22. Hence, the indenter's volumetric-strain was evaluated and was plotted versus the kinetic-energy in Fig. 23 which correlates the maximum load, kinetic energy and volumetric strain.

Figures 24 and 25 presents the AE-signals (raw), where the initial impact is noticeable, its termination corresponding to the peak in the force curves are plotted in Fig. 20. The cumulative-energy has been determined using discrete-time windows of 20 μs, and the results are plotted in Fig. 26. Phases I - III are difficult to characterize despite Phase III's end could obviously be specified on each curve. Hence, the impact time was identified using in the load curve (Fig. 20), and the area up to maximum load was evaluated and plotted versus the AE (cumulative) up to same time for maximum load, as shown in Fig. 27. The return-time (t_4) is plotted versus kinetic-energy in Fig. 28. These remarks illustrate that the relationship between the impact energy and AE energy is

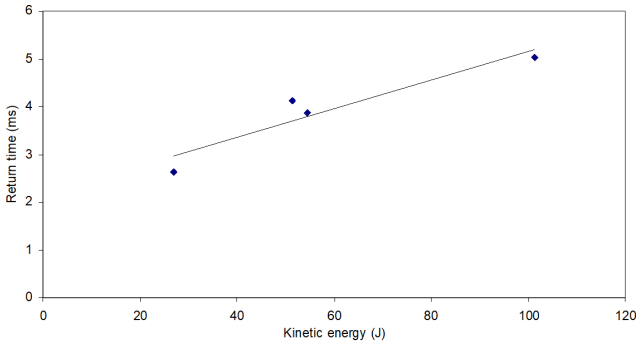

FIGURE 28. Kinetic-energy and return-time (t_4) via the conical-indenter.

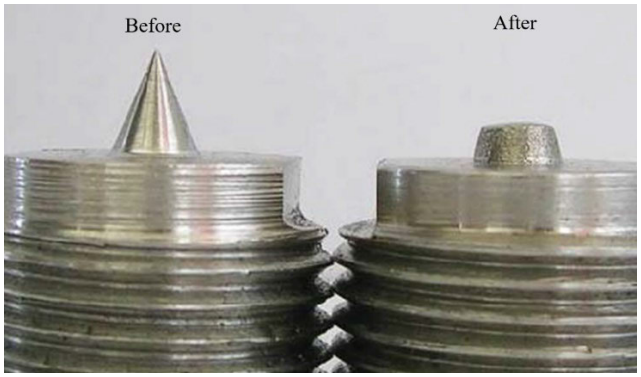

FIGURE 29. Indenter-shape prior and post the five impacts.

a bit complex. The anticipated relationship between kinetic-energy, volumetric-strain and impulsive-force, appears only for the drop-levels, indicating an uncontrolled experimental variable influencing the AE-energy. This could include uncontrolled loss of the sensor-coupling as a result of the impact or, possibly an inconsistent coupling between the indenter and the surface of the metal, provided that most of the AE is generated in the indenter as opposed to that on the pipe for the spherical-indenter.

C. EFFECT OF INDENTER'S SHAPE

The aforementioned data shows clearly that the AE-signature of impact is influenced by tuning the indenter shape, as illustrated in Fig. 7b and Fig. 24. To study this effect, a new conical-indenter was plopped from the same level with the identical mass for five trials to manifest this effect. The indenter shapes prior and post the experiment appeared in Fig. 29. The effect of indenter-shape on the raw AE signal is shown in Fig. 30, where it is obvious that the density (if not the amplitude) of events for the first impact using the fresh conical-indenter is greater than that once the cone has been crushed, and the return-time is much shorter for the initial drop, because the crushing ingests energy. Fig. 31 demonstrates the AE (cumulative) evolution for initial drop to be qualitatively different from the remaining four drop tests, which all have a plateau after about 0.6 ms, regaining the slope after about 0.8 ms. The heights of the Phase IV plateau also seem to change between the tests, although there is no

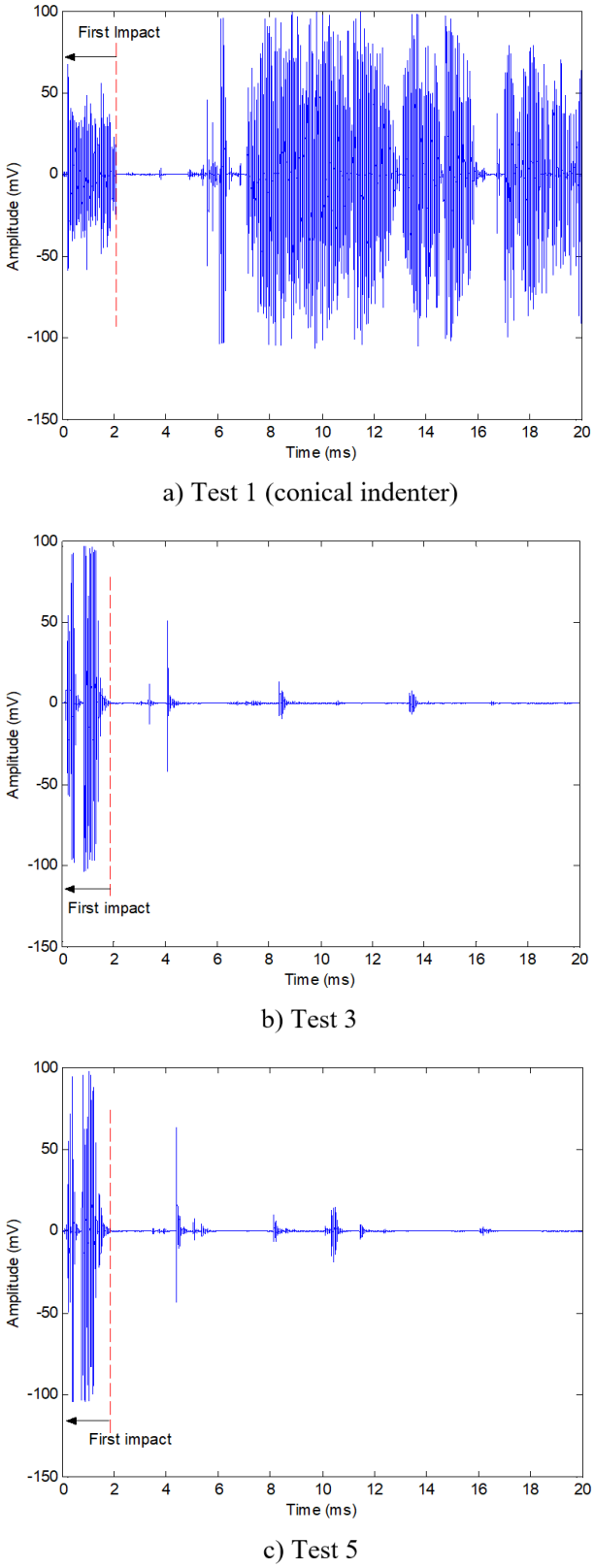

FIGURE 30. AE (raw) signals for 11.5 kg plopped from 1 m level via one indenter.

systematic order to the changes. It is therefore, concluded that, once an indenter has been used once, the contribution

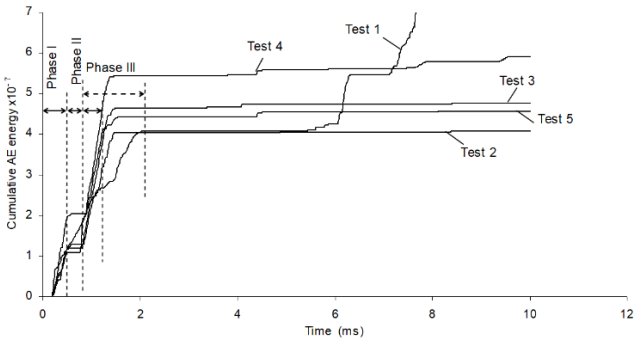

FIGURE 31. AE energy (cumulative) for 11.5 kg plopped from 1 m using one-indenter.

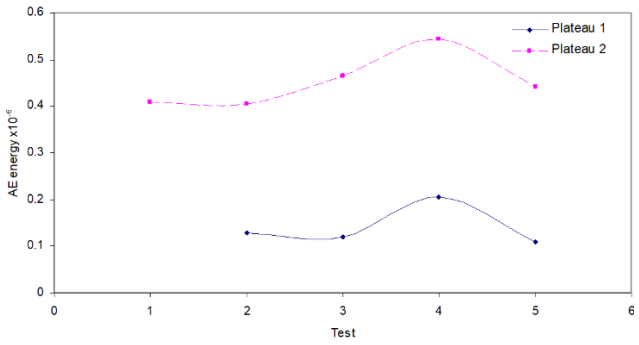

FIGURE 32. AE-energy for Phases I - III for the whole tests.

of crushing of the cone to the AE ceases to be significant in comparison with the contribution from deformation of the surface of the pipe. Fig. 32 shows the initial and subsequent plateaus for the cumulative AE evolutions shown in Fig. 31. It is clear that neither plateau shows a systematic change with the number of drops, although it is possible that the fourth drop shows the maximum combination of indenter crushing and surface determination. It is equally possible, however, that there is a variability in the results due to random effects.

IV. CONCLUSION

The focus of this study is to examine the behaviour of real sources where the sources are the impact of dropped weights. Analysis techniques are developed in to extract significant features of the AE signal associated with real sources, based mostly on techniques using energy in the time domain. The study has shown that temporal distribution of AE energy can reveal something about sources which are due to mechanical damage to the pipe. The detailed conclusions from the experiments involving dropped-weight impact are: -

- The AE-energy is influenced by the impact's kinetic-energy, however some dynamic effects in the experiments are deemed totally clarified.
- The AE-energy (cumulative) can be used to analyze the impact development with time.
- The impact's signatures could possibly be divided into four phases, and the last of these, Phase IV, apparently corresponding to loss of contact between the indenter and the surface for the levels and masses used in this work.
- The AE-signal (raw) in the dropped-mass test is affected by the indenter's shape, being dissimilar for new conical-indenters where the plastic-deformation is confined to the cone, and for the work-hardened indenters, where the plastic-deformation is mostly on the pipe surface.

REFERENCES

[1] M. Huang, L. Jiang, P. K. Liaw, C. R. Brooks, R. Seeley, and D. L. J. J. Klarstrom, "Using acoustic emission in fatigue and fracture materials research," *Jom*, vol. 50, no. 11, pp. 1–14, 1998.
[2] J. G. Scott, *Basic Acoustic Emission Nondestructive Testing* (Monographs and Tracts). New York, NY, USA: Gordon and Breach, 1991.
[3] M. Shehadeh, J. A. Steel, and R. L. Reuben, "Acoustic emission source location for steel pipe and pipeline applications: The role of arrival time estimation," *Proc. Inst. Mech. Eng., E, J. Process Mech. Eng.*, vol. 220, no. 2, pp. 121–133, May 2006.
[4] A. Ledeczi, T. Hay, P. Volgyesi, D.-R. Hay, A. Nadas, and S. Jayaraman, "Wireless acoustic emission sensor network for structural monitoring," *IEEE Sensors J.*, vol. 9, no. 11, pp. 1370–1377, Nov. 2009.
[5] H. Mei, M. Haider, R. Joseph, A. Migot, and V. Giurgiutiu, "Recent advances in piezoelectric wafer active sensors for structural health monitoring applications," *Sensors*, vol. 19, no. 2, p. 383, Jan. 2019.
[6] M. F. Shehadeh, "Monitoring of long steel pipes using acoustic emission," Ph.D. dissertation, School Eng. Phys. Sci., Mech. Eng., Heriot-Watt Univ., Edinburgh, U.K., 2006.
[7] A. Nasiri, J. Bao, D. Mccleeary, S.-Y. M. Louis, X. Huang, and J. Hu, "Online damage monitoring of SiC_f-SiC_m composite materials using acoustic emission and deep learning," *IEEE Access*, vol. 7, pp. 140534–140541, 2019.
[8] L. Pazdera, R. Dvoák, M. Hoduláková, L. Topolá, K. Mikuláek, J. Smutny, and Z. Chobola, "Application of acoustic emission method and impact echo method to structural rehabilitation," *Key Eng. Mater.*, vol. 776, pp. 81–85, Aug. 2018.
[9] M. R. Kaphle, "Analysis of acoustic emission data for accurate damage assessment for structural health monitoring applications," Ph.D. dissertation, Dept. Sci. Eng., School Chem., Phys. Mech. Eng., Queensland Univ. Technol., Brisbane, QLD, Australia, 2012.
[10] S. Shi, Z. Han, Z. Liu, P. Vallely, S. Soua, S. Kaewunruen, and M. Papaelias, "Quantitative monitoring of brittle fatigue crack growth in railway steel using acoustic emission," *Proc. Inst. Mech. Eng., F, J. Rail Rapid Transit*, vol. 232, no. 4, pp. 1211–1224, Apr. 2018.
[11] M. Wevers, "Listening to the sound of materials: Acoustic emission for the analysis of material behaviour," *NDT E Int.*, vol. 30, no. 2, pp. 99–106, Apr. 1997.
[12] H. Vallen, "AE testing fundamentals, equipment, applications," *NDT E Int.*, vol. 7, no. 9, pp. 1–30, 2002.
[13] W. A. Megid, M.-A. Chainey, P. Lebrun, and D. Robert Hay, "Monitoring fatigue cracks on eyebars of steel bridges using acoustic emission: A case study," *Eng. Fract. Mech.*, vol. 211, pp. 198–208, Apr. 2019.
[14] S. R. Saufi, Z. A. B. Ahmad, M. S. Leong, and M. H. Lim, "Low-speed bearing fault diagnosis based on ArSSAE model using acoustic emission and vibration signals," *IEEE Access*, vol. 7, pp. 46885–46897, 2019.
[15] S. Kim, "Impact damage classification using acoustic emission in composite structures," Ph.D. dissertation, Univ. Utah, Salt Lake, UT, USA, 2018. [Online]. Available: https://www.proquest.com/openview/85efde58fba8a8c147ddfbdd263a64d2/1.pdf?pq-origsite=gscholar&cbl=18750&diss=y
[16] K. G. Buckely Venkatesan, D. West, and M. Kaveh, "Detection and characterization of cracks for failure monitoring and diagnostics," in *Proc. IEEE Int. Conf. Acoust., Speech, Signal Process. Conf.*, vol. 5, Atlanta, GA, USA, May 1996, pp. 2738–2741.
[17] A. I. F. Robertson, R. Douglas, P. Nivesrangsan, E. Brown, J. Steel, and R. Reuben, "Source identification using acoustic emission on large bore cylinder liners," in *Proc. 26th Eur. Conf. AE Test.*, Berlin, Germany, 2004, pp. 637–643.
[18] P. Nivesrangsan, C. Cochrane, J. A. Steel, and R. L. Reuben, "AE mapping of engines for spatially-located time series," in *Proc. 25th Eur. Conf. AE Test.*, vol. 2, Prague, Czech Republic, 2002, pp. 1151–1158.

[19] P. Nivesrangsan, J. A. Steel, and R. L. Reuben, "AE mapping of engines for spatially located time series," *Mech. Syst. Signal Process.*, vol. 19, no. 5, pp. 1034–1054, Sep. 2005.
[20] M. G. Lozev, "Acoustic emission monitoring of steel bridge members," Transp. Res. Council, Virginia, Richmond, Tech. Rep. VTRC 97-R13, 1997.
[21] B. R. A. Wood and R. W. Harris, "Structural integrity and remnant life evaluation of pressure equipment from acoustic emission monitoring," *Int. J. Pressure Vessels Piping*, vol. 77, nos. 2–3, pp. 125–132, Feb. 2000.
[22] J. von Stebut, "Multi-mode scratch testing—A European standards, measurements and testing study," *Surf. Coatings Technol.*, vol. 200, nos. 1–4, pp. 346–350, Oct. 2005.
[23] J. W. R. Boyd and J. Varley, "The uses of passive measurement of acoustic emissions from chemical engineering processes," *Chem. Eng. Sci.*, vol. 56, no. 5, pp. 1749–1767, 2001.
[24] H. Richter, J. Böhmert, and H.-W. Viehrig, "The use of acoustic emission to determine characteristic dynamic strength and toughness properties of steel," *Nucl. Eng. Des.*, vol. 188, no. 2, pp. 241–254, Apr. 1999.
[25] K. Asamene, L. Hudson, and M. Sundaresan, "Influence of attenuation on acoustic emission signals in carbon fiber reinforced polymer panels," *Ultrasonics*, vol. 59, pp. 86–93, May 2015.
[26] D. G. Aggelis and T. E. Matikas, "Effect of plate wave dispersion on the acoustic emission parameters in metals," *Comput. Struct.*, vols. 98–99, pp. 17–22, May 2012.
[27] P. Sedlak, Y. Hirose, S. A. Khan, M. Enoki, and J. Sikula, "New automatic localization technique of acoustic emission signals in thin metal plates," *Ultrasonics*, vol. 49, no. 2, pp. 254–262, Feb. 2009.
[28] M. Shiwa, H. Yamawaki, H. Masuda, K. Ito, and M. Enoki, "AE signals analysis during chloride droplet SCC on thin plate of SUS304 steel," *Strength, Fract. Complex.*, vol. 5, nos. 2–3, pp. 109–116, 2009.
[29] M. Y. Bhuiyan and V. Giurgiutiu, "The signatures of acoustic emission waveforms from fatigue crack advancing in thin metallic plates," *Smart Mater. Struct.*, vol. 27, no. 1, Jan. 2018, Art. no. 015019.
[30] K. Ito, H. Yamawaki, H. Masuda, M. Shiwa, and M. Enoki, "SCC monitoring of chloride droplets on thin SUS304 plate specimens by analysis of continuous recorded AE waveform," *Mater. Trans.*, vol. 1, Aug. 2010, Art. no. 1007051111.
[31] T. C. Lindley, I. G. Palmer, and C. E. Richards, "Acoustic emission monitoring of fatigue crack growth," *Mater. Sci. Eng.*, vol. 32, no. 1, pp. 1–15, Jan. 1978.
[32] M. N. Bassim and M. Houssny-Emam, "Acoustic emission during the low cycle fatigue of AISI 4340 steel," *Mater. Sci. Eng.*, vol. 68, no. 1, pp. 79–83, Dec. 1984.
[33] C. E. Hartbower, C. F. Morais, W. G. Reuter, and P. P. Crimmins, "Acoustic emission from low-cycle high-stress-intensity fatigue," *Eng. Fract. Mech.*, vol. 5, no. 3, pp. 765–789, Sep. 1973.
[34] H. Montiel, J. A. Vílchez, J. Arnaldos, and J. Casal, "Historical analysis of accidents in the transportation of natural gas," *J. Hazardous Mater.*, vol. 51, nos. 1–3, pp. 77–92, Nov. 1996.
[35] A. M. Hedayetullah, "Optimization of indentification of particle impacts using acoustic emission," Ph.D. dissertation, Robert Gordon Univ., Aberdeen, U.K., 2018. [Online]. Available: https://rgu-repository.worktribe.com/output/248961/optimization-of-indentification-of-particle-impacts-using-acoustic-emission
[36] Y. Hu, G. Zhang, and Y. Yan, "Experimental investigations into the propagation of acoustic emission signals from particle impacts along a waveguide," *Sens. Actuators A, Phys.*, vol. 323, Jun. 2021, Art. no. 112651.
[37] N. Taberlet, J. Ferrand, M. H. Allah, B. Isnard, and N. Plihon, "Acoustic emission from successive impacts on elastic membranes: The physics of the screaming balloon," *EPL Europhys. Lett.*, vol. 126, no. 6, p. 64001, Jul. 2019.
[38] W. H. M. R. Prosser Gorman and D. H. Humes, "Acoustic emission signals in thin plates produced by impact damage," *J. Acoustic Emission*, vol. 17, nos. 1–2, pp. 29–36, 1999.
[39] L. Gaul and S. Hurlebaus, "Identification of the impact location on a plate using wavelets," *Mech. Syst. Signal Process.*, vol. 12, no. 6, pp. 783–795, Nov. 1998.
[40] Y. Ding, R. L. Reuben, and J. A. Steel, "A new method for waveform analysis for estimating AE wave arrival times using wavelet decomposition," *NDT E Int.*, vol. 37, no. 4, pp. 279–290, Jun. 2004.
[41] M. F. Shehadeh, M. Abdel-Geliel, and A. El-Araby, "Buckling detection within subsea pipeline laying using Acoustic Emission technique," in *Proc. 29th Eur. Conf. Acoustic Emission Test. (EWGAE)*, 2010, pp. 1–8.
[42] M. Abdel-Geliel, M. F. Shehadeh, and A. El-Araby, "Pipeline bending detection using Acoustic emission system," presented at the 17th Int. Congr. Sound Vib. (ICSV), 2010.
[43] M. Shehadeh, A. Osman, A. A. Elbatran, J. Steel, and R. Reuben, "Experimental investigation using acoustic emission technique for quasi-static cracks in steel pipes assessment," *Machines*, vol. 9, no. 4, p. 73, Mar. 2021.
[44] M. Shehadeh and M. Elghamry, "AE source location in long steel pipes using cross-correlation and wavelet transforms," in *Proc. 17th Congr. Condition Monitor. Diagnostic Eng. Manage.*, 2004, pp. 250–259.
[45] M. F. Shehadeh, A. H. Elbatran, A. Mehanna, J. A. Steel, and R. L. Reuben, "Evaluation of acoustic emission source location in long steel pipes for continuous and semi-continuous sources," *J. Nondestruct. Eval.*, vol. 38, no. 2, p. 40, Jun. 2019.
[46] L. Zhang, C. Enpei, G. Okudan, and D. Ozevin, "Phased acoustic emission sensor array for determining radial and axial position of defects in pipe-like structures," *J. Acoustic Emission*, vol. 36, pp. 1–2, Jun. 2019.
[47] L. Zhang, T. Zhang, E. Chen, D. Ozevin, and H. Li, "Phased acoustic emission sensor array for localizing radial and axial positions of defects in hollow structures," *Measurement*, vol. 151, Feb. 2020, Art. no. 107223.

MOHAMED SHEHADEH received the Ph.D. degree. He is currently the Dean of the Faculty of Engineering and Technology and a Professor with the Department of Mechanical and Marine Engineering, Arab Academy for Science, Technology and Maritime Transport, Egypt. He has many researches in marine, mechanical, and materials engineering. He is involved in many EU funded research projects, since 2008.

AHMED OSMAN received the Ph.D. degree from the Swinburne University of Technology, Melbourne, Australia. He is currently an Assistant Professor with the Marine Engineering Department, Arab Academy Science, Technology and Maritime Transport. His research interests include acoustic emission, corrosion engineering, materials engineering, marine, and offshore engineering. He has several international research collaborations especially in the Oceania and Asia-Pacific regions.

ALY HASSAN ABDELBAKY ELBATRAN received the B.Sc. and M.Sc. degrees from the Marine Engineering Department, AASTMT, Alexandria, Egypt, and the Ph.D. degree from the Department of Mechanical Engineering, Universiti Teknologi Malaysia (UTM), Malaysia. He is currently an Associate Professor with the Marine Engineering Department, and the Head of Mechanical Engineering Department, College of Engineering and Technology, Arab Academy for Science and Technology, South Valley Campus. He had participated in many European funds as well as works for ten years in design and research of mechanical and marine engineering fields. He has an academic background and deep research in the fields of renewable energy, hydrodynamics, CFD, and material engineering.

J. A. STEEL is currently the Head of the School of Engineering, Robert Gordon University. He is also the Chairperson of the Sand Management Network, which includes over 30 oil and gas companies, including operators and service companies. In recent years, he has been involved in research into monitoring and maintenance of offshore wind turbines as well as the applications of acoustic emission techniques to particles in flow and welding. He was a PI on a large EC Framework Programme 5 project in collaboration with Greek and Danish industrial and academic partners. This work has resulted in new ways of modeling AE wave transmission through complex mechanical objects, such as engines, and has enabled automatic identification of operating parameters and condition monitoring of components and processes in engines. Other research carried out in the group include modeling AE wave propagation on pipes and in composite plates, development of monitoring techniques in turbines, and monitoring of corrosion/erosion processes using AE.

R. L. REUBEN is an Emeritus Professor with the School of Engineering and Physical Sciences, Heriot-Watt University. He is also an Honorary Professor with the University of Edinburgh by virtue of his membership of the Edinburgh Research Partnership (EP) Joint Research Institute of Integrated Systems (JRI IIS). His research interests generally fall into the area of experimental mechanics, including: structure-property relationships for the development of engineering performance of materials and also for use as diagnostic indicators in medicine (tissue quality); development of new, quantitative approaches to analysis of stress waves in solids for diagnostic engineering; and the applications of mechanics to miniature mechanical systems to achieve real engineering solutions in millimetre-sized envelopes.